Combining Flyback and LLC Converters to Step Down Voltage from Battery in EV

Oda Byskov Aggerholm, s183700
DTU Electrical Engineering
31015 Introductory Project - Electrotechnology

Martin Ørskov Dieckmann Pedersen, s183702
DTU Electrical Engineering
31015 Introductory Project - Electrotechnology

***Abstract*—This paper describes the design of a 150 *W*, 145-200 *V* to 48 *V* converter for an EV realized by two series connected input capacitors, a flyback and an LLC converter. The design method and transformer design of the flyback and LLC converters are described. The converters are simulated in LTspice individually and combined using ideal components. Results are a theoretical model of a converter that delivers the desired voltage, including transformer designs with calculated power losses less than 6 *W*.**

I. Introduction

A new project at DTU Roadrunners is to build an electric car that runs on solar energy. The goal is to participate in the Bridgestone World Solar Challenge (BWSC) 2021. The car's battery must be able to supply energy to the motors as well as the electrical systems that use lower voltages. It is therefore relevant to be able to step down the voltage drawn from the battery. This paper describes the theoretical design of a converter that provides the desired voltage for the car's low voltage systems.

The design chosen to solve the task is shown in Fig. 1. It consists of two input capacitors connected in series, a flyback converter and an LLC converter. The combination of a flyback and LLC converter simplifies the design task compared to only using one type of converter. The idea of the two input capacitors is to let less power be transferred through the flyback converter to lower the total power loss. The specifications of the converter defined by the electrical team on the project are listed in Table I. As we want an output voltage of 48 V, it was decided that the input voltage of the LLC - and therefore also the voltage across C_{i2} - should be 96 V. As the voltage of the battery of the car will be 145-200 V, the voltage across C_{i1} will be 49-104 V. This results in 51-78 W transferred through the flyback converter.

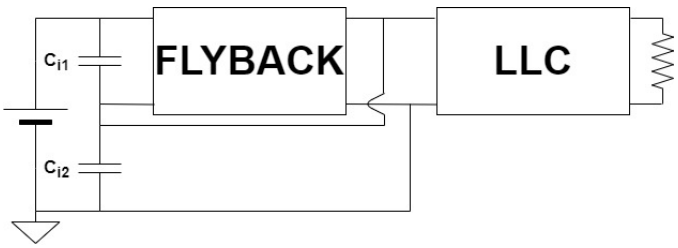

Fig. 1: Model of the designed converter.

TABLE I: Specifications of the converter.

Power	Input voltage	Output voltage
150 W	145-200 V	48 V

Regarding the rules of the competition, there are not any requirements concerning our design other than that the converter should be isolated so that you are not able to touch it [9]. This however, does not have any influence on the theoretical design of the circuits.

II. Flyback

The basic structure of a flyback converter consists of a switch, a transformer, a rectifying diode and an output capcitor. When the switch is on, the inductor on the primary side of the transformer is charged with a current that discharges through the inductor on the secondary side of the transformer, once the switch is turned off.

The purpose of the flyback converter in this design is to deliver a steady input voltage of 96 V to the LLC converter. As the battery of the vehicle will charge and discharge during the race, a variable input voltage of 49-104 V will be delivered to the flyback converter. A steady output voltage is ensured due to duty cycle control. This duty cycle control is achieved using a feedback loop that changes the duty cycle accordingly to the output voltage of the converter. The design of the control loop will not be performed.

A. Determining the Flyback Converter Parameters

As mentioned above, the output power of the entire converter should be 150 W. As only part of the power is transferred through the flyback, the power of the converter varies accordingly to the input voltage. By utilizing the fact that the ratio of the input power of the converter and the power of the flyback is proportional to the ratio of the input voltage of the converter and flyback respectively, the min/max power that the flyback should deliver was found

$$\frac{P_{flyback}}{P_{i,converter}} = \frac{V_{i,flyback}}{V_{i,converter}} \tag{1}$$

Based on [2] the switching frequency of the converter was chosen to be 100 kHz. The turn ratio and min/max duty cycle were determined using

$$\frac{V_o}{V_{in}} = n \cdot \frac{D}{1-D} \tag{2}$$

Thus leading to the parameters of the flyback converter specified in Table II.

TABLE II: Parameters of the Flyback Converter

Power assumption	50.69-78 W	
Duty cycle, D	24-40%	
Switching frequency, f	100 kHz	
Turn ratio, n	1:3	
	Min value	**Max value**
Input voltage, V_{in}	49 V	104 V
Input current, I_{in}	0.75 A	1.03 A
Output voltage, V_o	96 V	96 V
Output current, I_o	0.53 A	0.81 A

Using the approach in [1], the DC-component of the magnetizing current, I_M, was determined

$$I_M = n \cdot \frac{1}{1-D_{max}} \cdot I_{o,min} = 2.62\ A \tag{3}$$

As a rule of thumb, the magnetizing current ripple, di_M, is 25% of I_M

$$di_M = 0.25 \cdot I_M = 0.65\ A \tag{4}$$

causing a maximum value of the magmetizing current of $I_{M,max} = 3.27\ A$.

From [1] we got the magnetizing inductance, L_M, of the primary side of the transformer

$$L_M = \frac{V_{in,min} \cdot D_{max} \cdot f^{-1}}{2 \cdot di_M} = 147.8\ \mu H \tag{5}$$

The inductance of the secondary side was then given by $L_M \cdot n^2 = 1.33\ mH$.

The RMS-currents of the primary and secondary side of the transformer was determined using eq. 14.73 and 14.74 in [1]

$$I_{p,rms} = \frac{1}{n} \cdot I_M \cdot \sqrt{D_{max}} \cdot \sqrt{1 + \frac{1}{3} \cdot \left(\frac{di_M}{I_M}\right)^2} = 1.66\ A \tag{6}$$

$$I_{s,rms} = \frac{1}{n} \cdot I_M \cdot \sqrt{1-D_{max}} \cdot \sqrt{1 + \frac{1}{3} \cdot \left(\frac{di_M}{I_M}\right)^2} = 0.69\ A \tag{7}$$

B. Designing the Transformer

After trying out different cores and materials, the RM8/I-3C94-A400 core was chosen for the design. This core has an air gap length of $l_g = 0.2\ mm$, from which the number of primary turns could be determined from eq. 14.7 in [1]

$$L_M = \frac{\mu_0 \cdot A_e \cdot N_1^2}{l_g} \tag{8}$$

Where μ_0 is the relative permeability of free space, and $A_e = 63.0\ mm^2$ the effective area of the core. Using (8) the number of primary turns was set to $N_1 = 20$. The peak-to-peak value of the flux density, dB, was then found

$$dB = \frac{V_{in,min} \cdot D_{max} \cdot f^{-1}}{N_1 \cdot A_e} = 154\ mT \tag{9}$$

Hence the peak flux density of the core was given by $dB/2 = 77\ mT$, and the specific power loss, $P_v = 28\ kW/m^3$ could be read off Fig. 2.

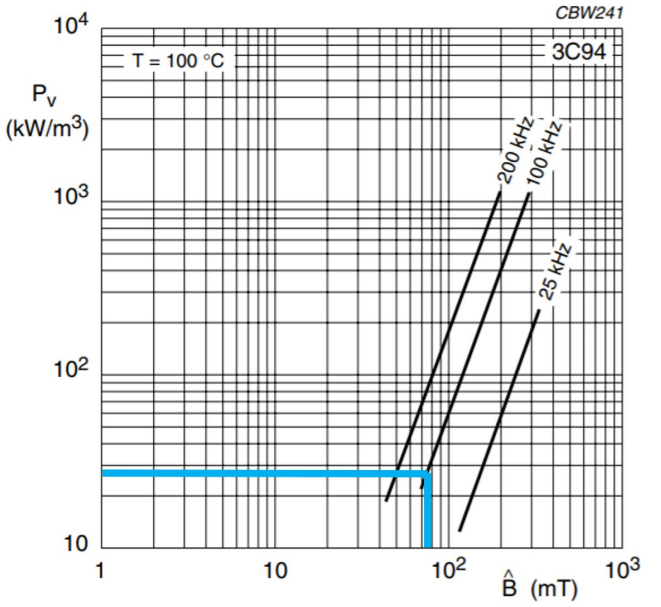

Fig. 2: Specific power loss of 3C94 as a function of peak flux density with frequency as a parameter [4].

Thus the core-loss

$$P_{core} = P_v \cdot V_e = 68.32\ mW \tag{10}$$

For the primary side of the transformer a wire with a diameter of $0.4\ mm$ was chosen as it satisfies that $I_{p,rms}/A_w < 15\ A/mm^2$. The DC-resistance of the wire, $R_{p,DC}$, could then be determined using eq. 14.13 in [1]

$$R_{p,DC} = \rho_{cu} \cdot \frac{N_1 \cdot MLT}{A_w} = 73.7\ m\Omega \tag{11}$$

where ρ_{cu} is the resistivity of copper, A_w is the cross-sectional area of the wire, and MLT the mean length per turn of the wire calculated from the dimensions of the core given in [3]. The winding width of the core $l_w = 10.8\ mm$. This means that there is room for 27 turns per layer. As there are 20 turns on the primary winding, only a single layer was needed - resulting in $MLT = 26.9\ mm/turn$.

The AC-resitance was calculated using the procedure on p. 515 in [1]

$$\delta = \sqrt{\frac{\rho_{cu}}{\pi \cdot \mu_0 \cdot f}} = 0.21\ mm \tag{12}$$

$$\eta = \sqrt{\frac{\pi}{4}} \cdot d \cdot \frac{n_l}{l_w} = 0.66 \tag{13}$$

$$\phi = \sqrt{\eta} \cdot \sqrt{\frac{\pi}{4}} \cdot \frac{d}{\delta} = 1.37 \tag{14}$$

Where δ is the skin depth, η the winding porosity, d the diameter of the wire, n_l the number of turns in a layer of width l_w, and ϕ a factor used to determine the resistance AC/DC ratio.

The AC/DC ratio of the resistance of the wire, $F_{R,p}$, was read off Fig. 3 to 1.3. Thus, the AC-resistance was determined to be

$$R_{p,AC} = F_{R,p} \cdot R_{p,DC} = 95.8\ m\Omega \tag{15}$$

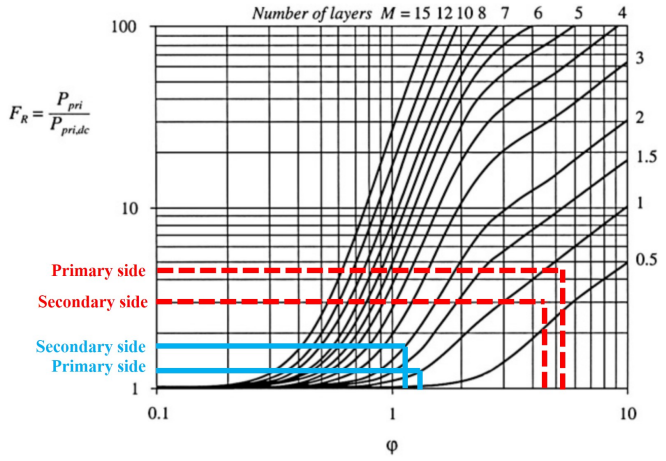

Fig. 3: Total winding copper loss as a function of ϕ and number of layers M [1]. The blue lines are for the flyback and the red, dotted lines are for the LLC.

The same method was used on the secondary side, where a wire with a diameter of 0.3 mm was chosen. This ment that there was room for 36 windings/layer - resulting in the need of 2 layers due to the 60 secondary windings. MLT was found to be 29.1 $mm/turn$. The DC and AC resistances of the wire were determined using (11) and (15) where $\eta = 0.89$ and $\phi = 1.20$ to: $R_{s,DC} = 425.3\ m\Omega$ and $R_{s,AC} = 722.9\ m\Omega$.

To calculate the total winding loss, it was necessary to determine the AC/DC contributions to the current

$$I_{p,DC} = I_M \cdot D_{max} = 1.03\ A \tag{16}$$

$$I_{p,AC} = \sqrt{(I_{p,rms})^2 - (I_{p,DC})^2} = 1.30\ A \tag{17}$$

$$I_{s,DC} = I_M \cdot (1 - D_{max}) = 1.58\ A \tag{18}$$

$$I_{s,AC} = \sqrt{(I_{s,rms})^2 - (I_{s,DC})^2} = 1.43\ A \tag{19}$$

Which gave a total copper loss

$$P_{cu} = I_{p,DC}^2 \cdot R_{p,DC} + I_{p,AC}^2 \cdot R_{p,AC} + I_{s,DC}^2 \cdot R_{s,DC} + I_{s,AC}^2 \cdot R_{s,AC} = 2.78W \tag{20}$$

Yielding in the total core and copper loss of the transformer

$$P_{total} = P_{core} + P_{cu} = 2.85\ W \tag{21}$$

From the dimensions of the core, the total winding area was found to be 91.3 mm^2. The area used in the design was 8.6 mm^2, why there is plenty of room for all the turns. Table III summarizes the properties of the designed transformer.

TABLE III: Summary of the Transformer

Core type	RM8/I
Material	3C94
Number of turns	N_1:N_2=20:60
Diameter of wire	N_1: 0.4 mm N_2: 0.3 mm
Core loss	0.06832 W
Copper loss	2.78 W
Frequency	100 kHz

C. Simulating the Flyback

As it was not possible to build a prototype of the converter, it was built and simulated in LTspice using ideal components. Fig. 4 shows the circuit in LTspice with minimum input voltage and maximum duty cycle. The circuit was tested for various input voltages and their corresponding duty cycles - all leading to the same results that are seen in Fig. 5. It is seen that the output stabilize after around 20 ms. Fig. 6 shows a closer view of the voltage and current waveforms.

Taking a look at Fig. 6 it is clear to see that the desired ouput voltage and current stated in Table II are obtained. The voltage ripple is $(96.4V - 95.94V)/96V = 0.9\%$ which is acceptable.

Fig. 6.b it shows that the calculated value of I_M and di_M are obtained as I_M can be read to be 2.6 A (halfway up the incline) meanwhile di_M is 0.7 A as the maximum and minimum values of the incline of I_M can be read to around 2 A and 3.3 A respectively. This is consistent with the calculation in (3). From the simulations the RMS-values of the currents of the transformer was moreover 1.66 A and 0.68 A, which is consistent with the values from equation (6) and (7).

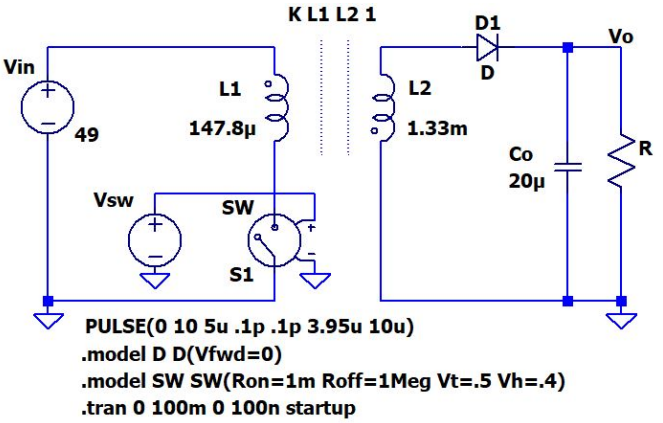

Fig. 4: LTspice model of the flyback converter with minimum input voltage.

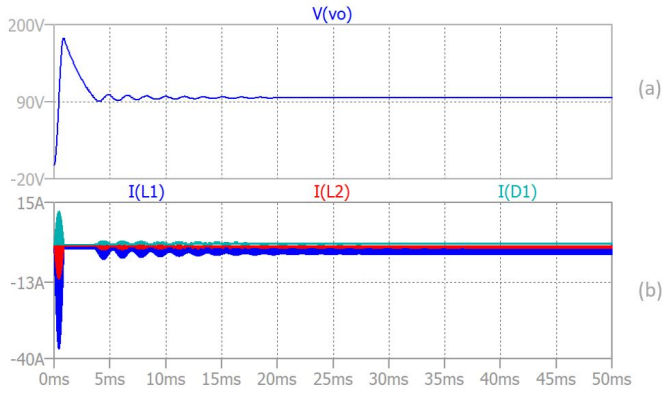

Fig. 5: Simulated values of (a) output voltage, and (b) output current (D1), current in the primary (L1) and secondary (L2) side of the transformer. The input voltage is 49 V.

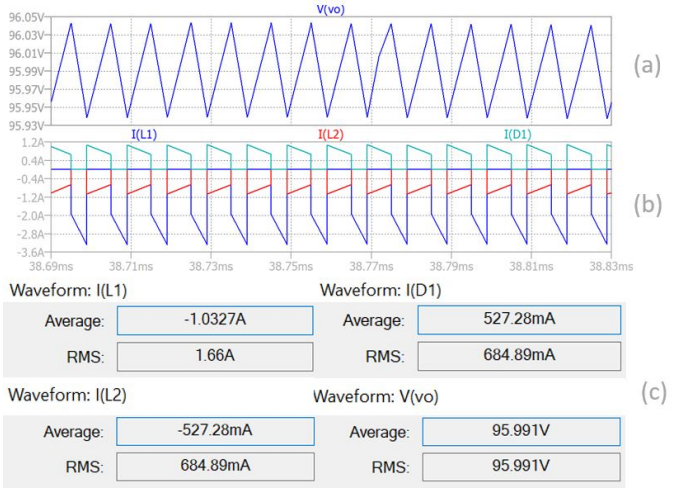

Fig. 6: (a), (b): Closer view of the waveforms in Fig. 5, (c): average and RMS values of the waveforms.

III. LLC

The LLC converter is a series resonant converter that consists of a half-bridge inverter, a resonant inductor L_r, a resonant capacitor C_r, a transformer with magnetizing inductance L_M, a full-wave diode rectifier and a capacitive output filter. Fig. 8 shows an LTspice model of the design.

The feature of the chosen design is to have the LLC operate at its resonant frequency, as this is the most efficient operating mode. The LLC was realized with the specifications: Power of 150 W, input voltage $V_{in} = 96\ V$ and output voltage $V_{out} = 48\ V$. Based on [6], a half-bridge and full-wave rectifier were chosen for the design. A half-bridge was used on the primary side as it requires fewer components, and the difference in conduction losses are lower than those of a full-bridge, due to the small primary side current. For the secondary side a full-wave rectifier was implemented since it is better suited for low voltage outputs and has fewer diodes compared to the full-bridge rectifier. The downside to these two choices is that the components need to be rated for higher voltages.

The magnetic inductance of the transformer was determined using the process proposed in [5], which ensures realization of zero voltage switching (ZVS). From this an expression that relates the magnetizing inductance to the device output capcitances, the dead time, and the switching period was derived. In ZVS the voltage curve across the switch does not overlap its current curve. This can be ensured by having enough dead time, T_d, for the voltage across the off-switch to drop to zero. This happens as the output capacitances, $C_{pri,oss}$, are discharged

$$I_{L_M,pk} T_d = 2 C_{pri,oss} V_{in} \tag{22}$$

For this project the transformer winding capacitance was not taken into account in the theoretical calculations. The desired peak voltage across the transformer is equal to V_{out} times the turn ratio, n, divided by 2. The peak current through the transformer occurs at the end of the on-cycle for switch 1, given by $T_s/2 - T_d$

$$I_{L_M,pk} = \frac{1}{L_M} \frac{nV_{out}}{2} \frac{(T_s/2) - T_d)}{1} \tag{23}$$

where T_s is the switching period, and the turn ratio is given by

$$n = \frac{V_{in}/2}{V_{out}} \tag{24}$$

Combining (22), (23) and (24) an expression for the magnetizing inductance was obtained

$$L_M = \frac{(T_d \cdot\ ((T/2) - T_d))}{(4 \cdot\ 2 \cdot C_{\text{oss pri}})} \tag{25}$$

The resonant inductor, L_r, was realized by utilizing the leakage inductance from the transformer, which is approximated to be 1% of the magnetic inductance. The impedance of the resonant capacitor, C_r, and L_r are the same at resonant frequency, hence the capacitance of C_r can be found by solving the equation

$$f_r = \frac{1}{2\pi\sqrt{C_r L_r}}. \tag{26}$$

A. Determining the LLC Parameters

A MOSFET [10] that has an output capacitance $C_{pri,oss} = 125\ pF$ was chosen, and $T_d = 100\ ns$ was selected. From these parameters along with (25) and (26) the sizes of L_M, L_r, C_r and $I_{L_M,pk}$, were found:

$L_M = 90\ \mu F$, $L_r = 0.9\ \mu F$, $C_r = 112\ nF$, $I_{L_M,pk} = 0.24\ A$.

In [5] expressions for the RMS currents of the primary and secondary sides are derived

$$I_{rms,p} = \sqrt{\frac{V_{out}^2 T_s^2 \pi^2}{8 R_L^2 n^2 (T_s - 2T_d)^2} + \left(\frac{1}{2} + \frac{2T_d}{T_s}\right) I_{L_m,pk}} \tag{27}$$

$$I_{rms,s} = n\sqrt{\frac{T_s - 2T_d}{2T_s}\left[I_{rms,p}^2 + \left(\frac{1}{3} - \frac{8}{\pi^2}\right) I_{L_m,pk}\right]} \tag{28}$$

which for this design was equal to $I_{rms,p} = 3.85\ A$ and $I_{rms,s} = 2.58\ A$.

B. Designing the Tranformer

The same procedure as for the flyback was used in the transformer design of the LLC. The design parameters and intermediate results towards the final transformer design are given in Table IV.

The core RM10/ILP with material 3F4 was chosen for the design. To achieve the lowest losses, a low number of turns were needed to get a higher flux. This resulted in $N = 10$ turns for the three windings. As the LLC is driven at a fixed switching frequency the expression for the peak-to-peak flux density dB is

$$dB = \frac{V_{in}(T_s/2 - T_d)}{NA_e} = 87.2\ mT \tag{29}$$

where A_e is the effective area of the core [7]. Hence, the peak flux density is $dB/2 = 43.6\ mT$. The specific power loss was then read off the graph in Fig. 7 to be $P_v = 150\ kW/m^3$, resulting in the total core loss

$$P_{core} = P_v \cdot V_e = 504\ mW \tag{30}$$

where V_e is the effective volume of the core.

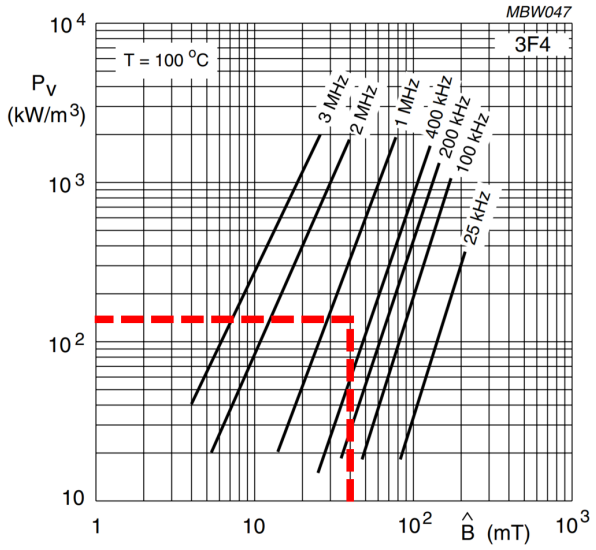

Fig. 7: Specific power loss of RM10 as a function of flux density with frequency as a parameter [7].

From the values in Table IV, as well as $I_{DC} = I_{Lm,pk}$ and I_{AC} calculated using (17), the total copper loss was found

$$P_{cu} = I_{p,DC}^2 \cdot R_{p,DC} + I_{p,AC}^2 \cdot R_{p,AC} + I_{s,DC}^2 \cdot R_{s,DC} + I_{s,AC}^2 \cdot R_{s,AC} = 2.16\ W \tag{31}$$

Adding this to P_{core} yielded a total power loss for the LLC transformer of $P_{loss} = 2.67\ W$.

TABLE IV: LLC Transformer Design Parameters

Parameter	Primary Winding	Secondary Winding
Wire diameter, d_{wire}	$0.6\ mm$	$0.5\ mm$
MLT	$37.1\ mm$	$37.1\ mm$
Skin depth, δ	$0.093\ mm$	$0.093\ mm$
Layer width, l_w	$6.7\ mm$	$6.7\ mm$
Turns per layer, n_l	11	13
Layers, M	1	1
Winding porosity, η	0.87	0.87
Phi, ϕ	5.3	4.3
AC/DC ratio, F_R	4.5	3
DC-resistance, R_{DC}	$22.6\ m\Omega$	$32.5\ m\Omega$
AC-resistance, R_{AC}	$101.7\ m\Omega$	$97.6\ m\Omega$
DC I_{DC}	$0.24\ A$	$0.24\ A$
AC I_{AC}	$3.85\ A$	$2.58\ A$

C. Simulating the LLC

The LLC was simulated using a voltage controlled ideal switch with an output capacitor and diode in parallel to model the chosen MOSFET. The switches in Fig. 8 are labeled with drain (D), source (S) and gate (G) to clarify how the MOSFET was modelled.

Fig. 9 shows the results from the simulation of the LLC. The top pane shows the output voltage. It settles after around $80\ \mu s$ after which it deviates less than 1% from $48\ V$. The two lower panes in Fig. 9 show the currents. When comparing the theoretical currents to the currents obtained in the simulation, it is seen that the theoretical values are lower than the simulated. The simulated primary side RMS current is 7.8% below the expected value. The simluated sencondary side RMS current is 4.7% below the expected value. Not quite acceptable, however the simulated $I_{L_M,pk}$ is $0.26\ A$ and the calculated was $0.24\ A$. These deviations might be caused by how the switches and the transformer are modelled, as they are not completely ideal. The lower RMS-currents in the simulation minimize the dead-time thus challenging the circuit's ability to realize ZVS. However, in the second top pane it can be seen that ZVS is realized, only with a smaller margin.

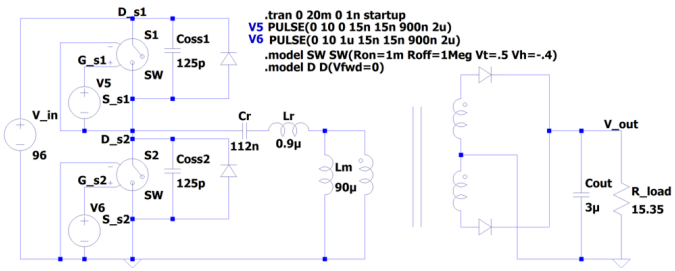

Fig. 8: LLC schematic for simulation.

IV. Complete Circuit

After testing the flyback and LLC converters individually, they were combined in the circuit design shown in Fig. 1. Some values were chosen for C_{i1} and C_{i2} and the circuit was simulated in LTspice.

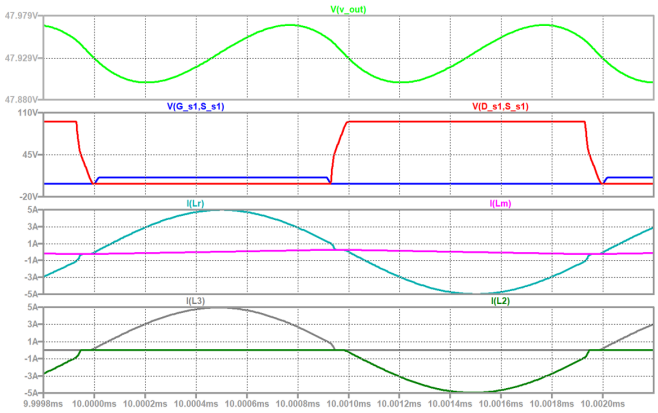

Fig. 9: Simulation measurements for the LLC converter.

In Fig. 10 the simulated values of the input capacitor voltages, output voltage and output power are shown. The output voltage ripple is given by $(47.740V - 47.675V)/48V = 0.15\%$ which is below 5% and therefore acceptable. From the figure it is clear to see that the voltages behave as required. The inductor currents are as in the simulations in the previous sections and are therefore not included here.

A significant problem, when simulating the complete circuit, is the lack of ZVS in the LLC switches. As seen in Fig. 10 the LLC gets the same input as in the isolated simulation, why it is strange that it behaves differently. We were however not able to figure out why. Apart from this, the combined simulation does behave accordingly to the isolated ones as described above.

Based on the fact that the transformers of the two converters are the greatest contributers to the power loss, the efficiency of the converter will be approximately

$$\frac{150\ W - P_{loss,flyback} - P_{loss,LLC}}{150\ W} = 96.3\% \qquad (32)$$

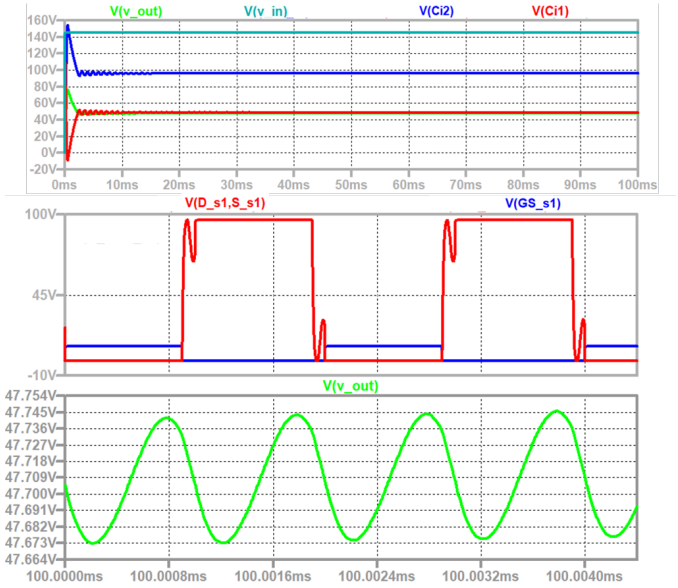

Fig. 10: Simulation of the complete circuit.

V. Conclusion

The designed converter is working as expected from a theoretical point of view on most parameters. An important thing to consider is figuring out how to ensure that ZVS is achieved in the converter, as this is an important design parameter concerning the efficiency of the LLC converter.

What is next to be done, is building a prototype to test how the design is behaving in reality. It will be necessary to make changes to existing component values as well as determining the components ensuring the right functionality of the ICs as for instance the feedback loop of the flyback.

The process of this project has shown that designing switch-mode converters is a tedious task that requires a lot of time for calculations, transformer design and testing. Moreover, it has illustrated that adjustments of project strategy can be necessary as problems occur - both from outide parameters and from within.

Acknowledgments

A special thanks should be given to Mingxiao Li for consistent help and guidance throughout the process of this project.

References

[1] Robert W. Erickson, and Dragan Maksimovic. *Fundamentals of Power Electronics*, 2nd edition. Chapters 13, 14, and 15. Kluwer Academic Publishers, 2004.

[2] Mingxiao Li, Arlene Meidahl, Sarah Hooper, and Yi Dou. *Solar Powered Laptop Charger*. Report: 31352 Power Electronics. DTU, December 2016.

[3] *Datasheet RM8/I*. Ferroxcube, September 2004. [Online]. Available from: http://ferroxcube.home.pl/prod/assets/rm8i.pdf. [Accessed June 2020].

[4] *Datasheet 3C94 Material Specification*. Ferroxcube, September 2004. [Online]. Available from: https://www.ferroxcube.com/upload/media/product/file/MDS/3c94.pdf. [Accessed June 2020].

[5] W. Zhang, F. Wang, D. J. Costinett, L. M. Tolbert, and B. J. Blalock, *Investigation of Gallium Nitride Devices in High-Frequency LLC Resonant Converters,* IEEE Trans. Power Electron., vol. 32, no. 1, pp. 571–583, 2017, doi: 10.1109/TPEL.2016.2528291.

[6] S. Abdel-Rahman, *Resonant LLC Converter: Operation and Design,* Appl. Note, AN2012-09, vol. 1.0, no. September, pp. 1–19, 2012.

[7] *Datasheet RM10/ILP*. Ferroxcube, September 2004. [Online]. Available from: https://www.ferroxcube.com/upload/media/product/file/Pr_ds/RM10_ILP.pdf. [Accessed June 2020].

[8] *Datasheet 3F4 Material Specification*. Ferroxcube, September 2004. [Online]. Available from: https://www.ferroxcube.com/upload/media/product/file/MDS/3f4.pdf. [Accessed June 2020].

[9] *2019 Regulations*. Bridgestone World Solar Challenge, October 2018.

[10] *Datasheet Power MOSFET AUIRFR4620*. Infenion, December 2015. Available from: https://datasheetspdf.com/pdf-file/1084193/Infineon/AUIRFR4620/1. [Accessed June 2020].

Problem Description

A new project at DTU Roadrunners is to build an electric car that runs on solar energy. The goal is to participate in the Bridgestone World Solar Challenge (BWSC) 2021. The car's battery must be able to supply energy to the motors as well as the electrical systems that use lower voltages. It is therefore relevant to be able to step down the voltage drawn from the battery. This project focuses on providing the right voltage for the car's electrical systems that use voltages significantly lower than the battery's. We will therefore investigate:

- How can you downgrade the voltage of the battery of the vehicle?
- Which rules and security measures must be kept?
- What specifications must be met so that the design fits the solar vehicle in the best possible way?
- The solution found must be tested to the extent possible.